# Bohm Criterion of Plasma Sheaths away from Asymptotic Limits

Yuzhi Li[1], Bhuvana Srinivasan[1], Yanzeng Zhang[2] and Xian-Zhu Tang[2]

[1]*Kevin T. Crofton Department of Aerospace and Ocean Engineering, Virginia Tech, Blacksburg, Virginia 24060, USA*
[2]*Theoretical Division, Los Alamos National Laboratory, Los Alamos, New Mexico 87545, USA*

The plasma exit flow speed at the sheath entrance is constrained by the Bohm criterion. The so-called Bohm speed regulates the plasma particle and power exhaust fluxes to the wall, and it is commonly deployed as a boundary condition to exclude the sheath region in quasineutral plasma modeling. Here the Bohm criterion analysis is performed in the intermediate plasma regime away from the previously known limiting cases of adiabatic laws and the asymptotic limit of infinitesimal Debye length in a finite-size system, using the transport equations of an anisotropic plasma. The resulting Bohm speed has explicit dependence on local plasma heat flux, temperature isotropization, and thermal force. Comparison with kinetic simulations demonstrates its accuracy over the plasma-sheath transition region in which quasineutrality is weakly perturbed and the Bohm criterion applies.

Sheath theory has a central place in plasma physics as its original formulation coincided with the recognition of plasma physics as a subfield in physics [1,2] and it applies to any plasma bounded by a material boundary [3–7]. One of the most celebrated findings in sheath theory is the so-called Bohm criterion [8–14] that predicts a threshold, the so-called Bohm speed, which would provide a lower bound for the plasma exit flow speed at the sheath entrance. Bohm criterion (also known as sheath criterion in the literature) is an inequality at the sheath entrance, which can be written as [9]

$$\left(\frac{\partial n_e}{\partial \phi} - Z\frac{\partial n_i}{\partial \phi}\right)\Bigg|_{\phi=\phi^{\text{se}}} \geq 0. \qquad (1)$$

Here $n_{e,i}$ denote the electron and ion density, respectively, $\phi$ is the plasma potential, and the superscript *se* labels the sheath entrance where the plasma transitions from quasineutral in the presheath to non-neutral inside the sheath. A straightforward [8,9], but not necessarily unique [10,11], physics interpretation of Bohm criterion is that Eq. (1) is required for the plasma potential to have non-oscillatory solutions into the sheath. This can be understood by linearizing the Poisson equation for $\phi$ in the neighborhood of the sheath entrance where $n_e \approx Zn_i$ remains a good approximation. The solution is of an exponential form with the exponent imaginary if Eq. (1) is violated, indicating an oscillatory $\phi$ into the sheath, which would contradict the expectation of monotonically varying $\phi$ that slows down the electrons for ambipolarity [9].

Traditionally, evaluation of Bohm speed from the Bohm criterion invokes drastic simplification of plasma transport. These are normally expressed in terms of varying $\gamma$ in the adiabatic law $pn^{-\gamma} = $ const. For example, $\gamma = 1$ for an isothermal plasma, $\gamma = 5/3$ for an ideal plasma having three degrees of freedom, and $\gamma = 3$ for an ideal plasma constrained to 1 degree of freedom. The Bohm speed in these limiting cases then equals the sound speed [11]

$$u_{\text{Bohm}} = c_s(\gamma_e, \gamma_i) \equiv \sqrt{(\gamma_e T_e^{\text{se}} + \gamma_i T_i^{\text{se}})/m_i}. \qquad (2)$$

It is interesting to note that although Bohm [8] originally invoked the isothermal electron approximation to realize the $\gamma_e = 1$ case of Eq. (2), subsequent work [15] had relaxed the requirement to a Boltzmann distribution for the electron density, $n_e = n_0 \exp(e\phi/T_e^*)$, with $\phi$ the plasma potential and $T_e^*$ an effective or screening temperature, the latter of which is interpreted as what Langmuir probes are supposed to measure.

It was recognized early on Ref. [9] that transport in the neighborhood of the sheath can greatly complicate the physics constraint set by the Bohm criterion. A large body of work [10,11,16–18] has since been devoted to the development of the so-called kinetic Bohm criterion, which is obtained by integrating the kinetic equation for $n_{i,e}$ in Eq. (1). The standard expression bears the form

$$\frac{1}{m_i}\int d^3\mathbf{v}\,\frac{f_i(\mathbf{v})}{v_z^2} \leq -\frac{1}{m_e}\int d^3\mathbf{v}\,\frac{1}{v_z}\frac{\partial f_e(\mathbf{v})}{\partial v_z}, \qquad (3)$$

with $m_i(m_e)$ the ion (electron) mass, $f_i(f_e)$ the ion (electron) distribution function, and velocity $v_z$ which is normal to the wall in an unmagnetized plasma or parallel to the magnetic field in a magnetized plasma. A recent debate [12,19,20] highlighted a profound disconnect between (i) the conventional theory of the Bohm criterion and (ii) the practical needs in plasmas that we normally

encounter. Specifically, the Bohm criterion like in Eq. (3) was derived in the asymptotic limit of $\lambda_D/L \to 0$ [19] with $\lambda_D$ the Debye length and $L$ the plasma size, while plasmas of practical interest are frequently away from this asymptotic limit [20]. The underlying challenge echoes back to an earlier discussion [21–26] on where the sheath entrance or edge resides, an intimately connected issue since that is where the Bohm criterion is supposed to be applied.

The complication is that between the quasineutral plasma and the non-neutral Debye sheath in a plasma away from the asymptotic limit of $\lambda_D/L \to 0$, there is usually a transition layer in which the quasineutrality is weakly violated, and the plasma flow and potential (and its gradient and hence electric field) can vary gradually [25–28]. Matched asymptotic analysis of a simplified plasma model with isothermal electrons and cold ions, reveals that the plasma ion flow actually crosses the classically defined Bohm speed [8] $u_{\text{Bohm}} = \sqrt{T_e/m_i}$ somewhere inside this transition layer [26,27]. This is consistent with the straightforward interpretation of the Bohm criterion as given in Eq. (1) by Harrison and Thompson [9] that (i) it offers no meaningful constraint in the quasineutral region because $n_e \approx Zn_i$ and Poisson's equation is not used for evaluating $\phi$; (ii) it does not apply in the Debye sheath in the sense of Langmuir and Tonks [1,2] since $n_e$ grossly differs from $Zn_i$, and (iii) it does impose a constraint, as we shall show in this Letter, on the ion flow speed over the spatially extended transition region, as opposed to a sharp transition boundary, over which quasineutrality is mildly perturbed so charge density gradient is the dominant term upon linearization of Poisson's equation. This last point implies a Bohm speed that should vary inside this transition region.

In this Letter, we derive an expression for the Bohm speed away from the previously known asymptotic limits, that elucidates the distinct roles of various transport physics, including heat flux, collisional isotropization, and thermal force for both electron and ion transport. Its explicit dependence on plasma transport and local electric field suggests a spatially varying Bohm speed over a transition region in which quasineutrality is weakly perturbed. This is confirmed by first-principle kinetic simulations over a range of plasma collisionality. To our knowledge, this is the first time that a predictive formula for Bohm speed has been shown to be quantitatively accurate in the intermediate plasma regime that is away from the limiting cases of adiabatic laws and the asymptotic limit of $\lambda_D/L \to 0$.

The nature of plasma transport in the sheath and presheath region is governed by the sheath Knudsen number $K_n$, which is the ratio between plasma mean-free-path $\lambda_{mfp}$ and the Debye length $\lambda_D$. In cases of most interest, $K_n > 1$ or $K_n \gg 1$. A consequence is that within the Knudsen layer, which is defined as one mean-free-path ($\lambda_{mfp}$) within the wall, streaming loss and the associated

decompressional cooling would induce robust temperature anisotropy [29], $T_\parallel < T_\perp$. The parallel degree of freedom is along the magnetic field, or in an unmagnetized plasma the plasma flow direction, which is normal to the wall surface. Because of the anisotropic nature of the plasma, the mean-free-path is defined as $\lambda_{mfp} \equiv v_{\text{th},e}/\nu_{ei}$ with $v_{\text{th},e} = \sqrt{T_{e\parallel}/m_e}$ the electron thermal velocity and $\nu_{ei}$ the electron-ion collision frequency in an anisotropic plasma given by Eq. (7). Here we will focus on a magnetized plasma, with a uniform magnetic field normal to the wall ($T_\parallel = T_x$) and $y$ signifying a perpendicular direction ($T_\perp = T_y$). The plasma transport equations that directly enter the Bohm speed evaluation include the species continuity equation, momentum equation, and energy equation, all in the parallel or $x$ direction, which in the neighborhood of the sheath entrance, take the form,

$$\frac{\partial n_e u_{ex}}{\partial x} = 0; \qquad \frac{\partial n_i u_{ix}}{\partial x} = 0, \tag{4a}$$

$$\frac{\partial n_e T_{ex}}{\partial x} = en_e \frac{\partial \phi}{\partial x} - \alpha n_e \frac{dT_{ex}}{dx}, \tag{4b}$$

$$n_i m_i u_{ix} \frac{\partial u_{ix}}{\partial x} + \frac{\partial n_i T_{ix}}{\partial x} = -Zen_i \frac{\partial \phi}{\partial x} + \alpha n_e \frac{dT_{ex}}{dx}, \tag{4c}$$

$$n_e u_{ex} \frac{\partial T_{ex}}{\partial x} + 2n_e T_{ex} \frac{\partial u_{ex}}{\partial x} + \frac{\partial q_n^e}{\partial x} = Q_{ee} + Q_{ei}, \tag{4d}$$

$$n_i u_{ix} \frac{\partial T_{ix}}{\partial x} + 2n_i T_{ix} \frac{\partial u_{ix}}{\partial x} + \frac{\partial q_n^i}{\partial x} = Q_{ii}. \tag{4e}$$

Here we have ignored the electron inertia and a net plasma current into the wall, $\alpha$ is the thermal force coefficient, $q_n^{e,i}$ are the heat flux of $x$-degree of freedom in the $x$ direction,

$$q_n \equiv \int m(v_x - u_x)^3 f d^3\mathbf{v}, \tag{5}$$

and $(Q_{ee}, Q_{ei}, Q_{ii})$ are temperature isotropization terms in an anisotropic plasma, which in high collisionality limit [30] have the form,

$$Q_{ee,ei} = 8n_e \nu_{ee,ei} T_{ey} \frac{T_{ex}}{T_{ey} - T_{ex}} \left[ -3 + \left( 3\sqrt{\frac{T_{ex}}{T_{ey} - T_{ex}}} \right. \right.$$
$$\left. \left. + \sqrt{\frac{T_{ey} - T_{ex}}{T_{ex}}} \right) \arctan\sqrt{\frac{T_{ey} - T_{ex}}{T_{ex}}} \right], \tag{6}$$

with the collision rate

$$\nu_{ee} = \frac{\nu_{ei}}{Z\sqrt{2}} = \frac{\sqrt{\pi}}{2} n_e \frac{e^4}{(4\pi\varepsilon_0)^2} \frac{\ln\Lambda}{\sqrt{m_e T_{ex} T_{ey}}}. \qquad (7)$$

The evaluation of the Bohm speed can now be performed following Ref. [31]. Combining the electron continuity equation, momentum equation, and energy equation, we can substitute out the $\partial T_{ex}/\partial x$ and $\partial u_{ex}/\partial x$ terms and find that in the neighborhood of the sheath entrance where $\phi$ is a monotonically varying function of $x$,

$$\frac{\partial n_e}{\partial \phi} = \frac{e n_e}{(3+2\alpha)T_{ex}} + \frac{1+\alpha}{(3+2\alpha)u_{ex}T_{ex}}\left(\frac{\partial q_n^e}{\partial \phi} + \frac{Q_{ee}+Q_{ei}}{E}\right), \qquad (8)$$

where $E = -\partial\phi/\partial x$ is the electric field. In contrast, the ion inertia must be retained in a similar analysis of the ion continuity, momentum, and energy equations, and the result is

$$\frac{\partial n_i}{\partial \phi} = \frac{1}{3u_{ix}T_{ix} - m_i u_{ix}^3}\left(\frac{\partial q_n^i}{\partial \phi} + \frac{Q_{ii}}{E}\right) - \frac{Zen_i - \alpha n_e \partial T_{ex}/\partial\phi}{3T_{ix} - m_i u_{ix}^2}. \qquad (9)$$

Substituting Eqs. (8) and (9) into Eq. (1), and rearranging terms, we find that the Bohm criterion provides a lower bound for the plasma exit flow speed,

$$u_{ix}^{\mathrm{se}} \geq u_{\mathrm{Bohm}} \qquad (10)$$

with

$$u_{\mathrm{Bohm}} \equiv \sqrt{\frac{Z\beta T_{ex}^{\mathrm{se}} + 3T_{ix}^{\mathrm{se}}}{m_i}}, \qquad (11)$$

and

$$\beta \equiv \frac{3 - \frac{3+2\alpha}{Ze\Gamma_i^{\mathrm{se}}}\left(\frac{\partial q_n^i}{\partial \phi} + \frac{Q_{ii}}{E}\right) + \frac{\alpha}{e\Gamma_e^{\mathrm{se}}}\left(\frac{\partial q_n^e}{\partial \phi} + \frac{Q_{ee}+Q_{ei}}{E}\right)}{1 + \frac{1+\alpha}{e\Gamma_e^{\mathrm{se}}}\left(\frac{\partial q_n^e}{\partial \phi} + \frac{Q_{ee}+Q_{ei}}{E}\right)}. \qquad (12)$$

Here, $\Gamma_{e,i} = n_{e,i}u_{ex,ix}$, and all quantities on the right hand side of Eq. (12) are evaluated locally at the sheath entrance, which is interpreted here as the plasma-to-sheath transition region where quasineutrality is weakly violated.

The Bohm speed defined in Eqs. (11) and (12) takes into account the known collisional transport physics. It recovers the collisionless sheath-presheath limit previously found in Ref. [31], which is obtained by setting $\alpha$, $Q_{ee}$, $Q_{ei}$, and $Q_{ii}$ to zero,

$$\beta = \left(3 - \frac{3}{Ze\Gamma_i^{\mathrm{se}}}\frac{\partial q_n^i}{\partial \phi}\right) / \left(1 + \frac{1}{e\Gamma_e^{\mathrm{se}}}\frac{\partial q_n^e}{\partial \phi}\right). \qquad (13)$$

A particularly interesting limit is $L \gg \lambda_{mfp} \gg \lambda_D$ so the upstream plasma is a Maxwellian. The presheath-sheath

electrons follow a truncated bi-Maxwellian due to the trapping effect of the ambipolar electrostatic potential, which gives rise to an electron heat flux that satisfies $\partial q_n^e/\partial\phi = 2e\Gamma_e^{\mathrm{se}}$ [32]. Ignoring the much smaller ion heat flux, one then finds $u_{\mathrm{Bohm}} = \sqrt{(T_{ex} + 3T_{ix})/m_i}$ because of the dominant contribution from the electron heat flux term [31]. This strikes a remarkable but superficial coincidence with the Bohm speed expression in Eq. (2) for $c_s(\gamma_e = 1, \gamma_i = 3)$.

The full expression in Eq. (12) allows us to quantify the transport physics effect on Bohm speed over a wide range of plasma collisionality. Perhaps the subtlest factor is the collisional temperature isotropization. Naively, one would expect $Q_{ee}$ to be small when plasma collisionality is either strong in which case $T_y - T_x$ vanishes, or weak in which case $\nu_{ee}$ becomes negligibly small. This can be quantitatively assessed by expanding $Q_{ee}$ in the small parameter of $X \equiv \sqrt{(T_{ey} - T_{ex})/T_{ex}}$. To leading order in $X$, the collisional closure of Chodura and Pohl [30] predicts

$$Q_{ee} = \frac{32}{15} n_e \nu_{ee} T_{ey} X^2. \qquad (14)$$

The collisional temperature isotropization enters the Bohm speed with normalization by the electron flux and electric field at the sheath entrance,

$$\begin{aligned}\frac{Q_{ee} + Q_{ei}}{e\Gamma_e E} &\approx (1 + Z\sqrt{2})\frac{32}{15}\frac{n_e \nu_{ee} T_{ey} X^2}{en_e u_{ex} E} \\ &= (1 + Z\sqrt{2})\frac{32}{15}\frac{v_{th,e}}{u_{ex}^{\mathrm{se}}}\frac{\lambda_D}{\lambda_{mfp}}\frac{T_{ey}}{eE\lambda_D}X^2 \\ &\approx (1 + Z\sqrt{2})\frac{32}{15}\sqrt{\frac{T_{ex}^{\mathrm{se}}}{\beta T_{ex}^{\mathrm{se}} + 3T_{ix}^{\mathrm{se}}}}\frac{\sqrt{m_i/m_e}}{K_n}\frac{T_{ey}}{\lambda_D eE}X^2.\end{aligned} \qquad (15)$$

In the collisionless sheath limit $K_n \to \infty$ but all the other terms are bounded so

$$\lim_{K_n \to \infty}\frac{Q_{ee} + Q_{ei}}{e\Gamma_e E} = 0, \qquad (16)$$

which is the limiting result to be expected. In the intermediate regime of finite collisionality, different offsetting physics can produce an order-unity $(Q_{ee} + Q_{ei})/e\Gamma_e E$ that has an indispensable role in setting the Bohm speed. In the high collisionality regime, which is denoted by $K_n < \sqrt{m_i/m_e}$, the small but still finite temperature anisotropy is the offsetting factor that produces a $(Q_{ee} + Q_{ei})/e\Gamma_e E \sim O(1)$. With a decreasing collisionality so $K_n > \sqrt{m_i/m_e}$ but not too much greater, there are two offsetting factors coming into play. The first is the familiar temperature anisotropy, which can be enhanced by an order of magnitude. The second is a much reduced

electric field at the sheath entrance, which can boost the factor $T_{ey}/\lambda_D eE$. Overall, one finds that for a range in which $K_n > \sqrt{m_i/m_e}$, the two effects can offset a large $K_n$, so $(Q_{ee} + Q_{ei})/e\Gamma_e E$ remains order unity and hence has an important role in setting the Bohm speed.

Next we deploy first-principle kinetic simulations to verify the Bohm speed of Eqs. (11), (12) and quantify the relative importance of various transport physics under consideration. The VPIC [33] simulations are for a slab plasma bounded by absorbing walls at $x = 0$ and $x = L$. The loss at the wall is balanced by a plasma source in the middle $x \in [3/8L, 5/8L]$, as a way to mimic the upstream source for the scrape-off layer plasma in a tokamak. Other specifics include $L = 256\lambda_D$, $N = 10000$ markers per cell, $Z = 1$, $m_i/m_e = 1836$. The source temperatures $T_{e0} = T_{i0}$ and the background or initial plasma density $n_0$ will be varied so the sheath Knudsen number $K_n \in [20, 5000]$. The uniform magnetic field is strong so the plasma beta is much less than unity, ~1%. At the sheath entrance $K_n^{se}$ would be smaller, but proportional to $K_n$. There are three essential points we will focus on here [34].

The first point is on the sheath entrance, which for a plasma away from the asymptotic limit of $\lambda_D/L \to 0$, covers a transition region in which deviation from quasi-neutrality is small but finite. The transition into the sheath can be most obviously assessed by fractional charge density $|n_e - n_i|/(n_e + n_i)$, but a more sensitive measure for Bohm criterion is $|\partial n_e/\partial x - \partial n_i/\partial x|/(|\partial n_e/\partial x| + |\partial n_i/\partial x|)$. In Fig. 1, one can see that with the PIC noise of $N = 10000$ markers per cell, we can reliably position the edge of the sheath transition region to $x > 5\lambda_D$ using the charge density gradient, while the charge density itself gives a sensitivity to $x = 2.5\lambda_D$. The simulation data of the fractional charge density gradient, which has higher sensitivity, is consistent with a sheath transition region over which the violation of quasineutrality is small, and proceeds gradually towards the non-neutral Debye sheath.
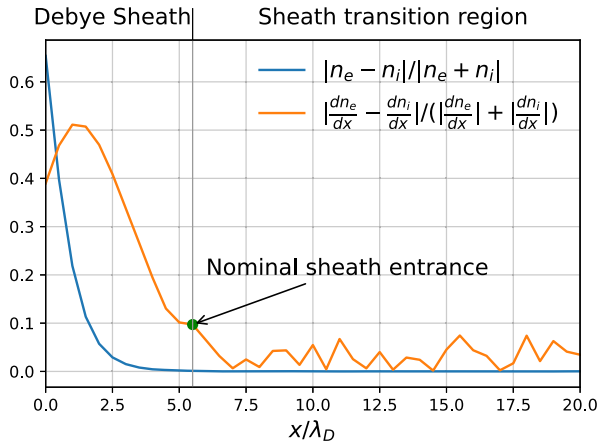
The second point is that over the spatially extended sheath transition region, the Bohm criterion should be applicable with a high degree of accuracy that is measured by the fractional change in charge density gradient. In Fig. 2, we contrast the ion flow speed from VPIC simulations, with the Bohm speed from Eqs. (11) and (12), as a function of position from the wall. Here, in evaluating the Bohm speed, we compute all individual terms in Eq. (12) using the VPIC simulation data. Since the terms in Eq. (12) involve higher-order velocity moments and their derivatives, we deploy time-averaging (but not spatio-averaging) over a long period in which the plasma has reached steady state. This overcomes the constraint of the normal PIC noise level of $1/\sqrt{N}$ with $N$ the particle markers per cell. The inherent PIC noise has been suffi-ciently suppressed that we can see a clear sheath transition region over which the ion flow speed closely follows the Bohm speed of Eqs. (11) and (12) in Fig. 2. Further into the Debye sheath, the ion flow speed diverges from the locally evaluated Bohm speed to become significantly greater, as expected. Further away from the Debye sheath and wall, the theoretical expectation is that Eqs. (11) and (12) would set a local Bohm speed as long as it is still within the transition region where quasineutrality is weakly perturbed. It must be emphasized that in the quasineutral region, the Bohm criterion as of Eq. (1) is not a viable concept, so Eq. (1) no longer produces a physically meaningful speed to constrain the ion flow.

The third point is on the relative importance of various transport physics in setting the Bohm speed. The transport under examination is collisional by nature, and includes thermal force, heat flux, and collisional temperature iso-tropization, for both electrons and ions. We are particularly interested in how these dependencies vary (a) with colli-sionality $K_n$ and (b) over space in the transition layer of a



FIG. 1. The normalized net charge density $\bar{\rho}$, and the fractional charge density gradient $\overline{\partial\rho/\partial x}$ for $K_n = 200$.
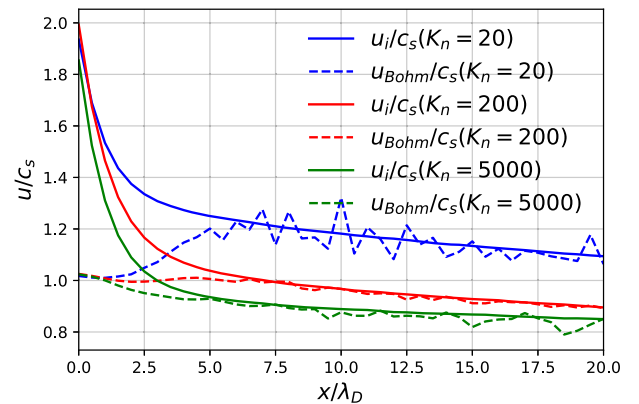


FIG. 2. Ion exit flow speed from simulation data and Bohm speed calculated from Eqs. (11) and (12) normalized by $c_s(\gamma_e = 1, \gamma_i = 3)$ in Eq. (2) over distance from wall for $K_n = 20, 200,$ and 5000. The breakdown of $u_{Bohm}$ from Eqs. (11) and (12) for Bohm speed is an accurate indication of transitioning into non-neutral Debye sheath.

TABLE I. Sheath quantities (columns) around the nominal sheath entrance ($x/\lambda_D$) for nominal [39] $K_n = (20, 200, 5000)$ cases (rows), with $K_n^{\rm se}$ the local Knudsen number.

| $K_n^{\rm se}$ | $x/\lambda_D$ | $u_{ix}/c_s$ | $u_{\rm Bohm}/c_s$ | $(1/e\Gamma_e^{\rm se})(\partial q_n^e/\partial\phi)$ | $[(Q_{ee}^{\rm se} + Q_{ei}^{\rm se})/e\Gamma_e^{\rm se}E^{\rm se}]$ | $(1/e\Gamma_i^{\rm se})(\partial q_n^i/\partial\phi)$ | $(Q_{ii}^{\rm se}/e\Gamma_i^{\rm se}E^{\rm se})$ | $\alpha^{\rm se}$ |
|---|---|---|---|---|---|---|---|---|
| 5.26 | 5.0 | 1.25 | 1.20 | $-1.63$ | 1.48 | $-0.05$ | 0.18 | 0.59 |
| 50.0 | 5.5 | 1.02 | 1.00 | $-2.20$ | 3.55 | $-0.22$ | 0.38 | 0.45 |
| 1932 | 5.0 | 0.94 | 0.93 | 0.23 | 1.17 | 0.52 | 0.07 | 0.04 |

given $K_n$. For (a), we contrast the ion flow speed with the Bohm speed at a nominal sheath entrance point for different nominal $K_n$ cases. The terms in Eq. (12) are computed from simulation data and separately tabulated in Table I to quantify their relative importance [36]. Also shown are the local sheath Knudsen number $K_n^{\rm se}$, ion exit flow speed $u_{ix}$ directly from simulations, and $u_{\rm Bohm}$ computed from Eqs. (11) and (12) using the tabulated data for each case. Both $u_{ix}$ and $u_{\rm Bohm}$ are normalized by $c_s(\gamma_e = 1, \gamma_i = 3)$ from Eq. (2), using $T_{ex}^{\rm se}$ and $T_{ix}^{\rm se}$ from the simulations. The electron thermal flux enters through a divergence in the energy equation, so it is a dominant term in sheath analysis [31]. This is clearly indicated by the data, with additional subtleties in the high $K_n$ limit that the whistler instability driven by trapped electrons [37] can modify the parallel electron thermal conduction flux in a magnetized plasma, and magnetic field strength modulation on sheath scale can also modify the parallel thermal flux [38]. As previously discussed after Eq. (15), the collisional electron temperature isotropization has an equally important role that is further aided by the decreasing local electric field (in magnitude) as $K_n$ increases. An accurate $E^{\rm se}$ was previously found by Kaganovich [23] to be important for matching the sheath solution to the quasineutral plasma in a two-scale analysis, here we find that it enters explicitly in the Bohm speed as well. Table I also reveals that despite the mass ratio in a hydrogen plasma, ion heat flux and ion temperature isotropization can have a small but appreciable contribution to the Bohm speed. Finally, the thermal force coefficient $\alpha^{\rm se}$ is directly measured from simulation data, and one can verify that Bohm speed has a very weak dependence on $\alpha^{\rm se}$ for $\alpha$ less than or equal to the Braginskii value. For (b), we have the remarkable finding that the heat flux gradient and collisional temperature isotropization terms vary substantially in the sheath transition layer, but together they produce a Bohm speed from Eqs. (11) and (12) that agrees accurately with simulated ion flow over space in Fig. 2. The detailed data for such a comparison is given in the Supplemental Material [34] for the $K_n = 200$ case.

In conclusion, we have derived an expression for the Bohm speed that is accurate over a broad range of plasma collisionality. The Bohm speed is derived from the transport equations of an anisotropic plasma, which is expected for the sheath transition problem. This expression is verified by comparison with first-principle kinetic simulations, within the bounds set by the PIC noise. Of particular interest is that the Bohm speed thus formulated applies to the sheath transition region in which the quasineutrality is weakly perturbed. This, to our knowledge, is the first time that a predictive formula for Bohm speed has been shown to be quantitatively accurate in the intermediate plasma regime, which is away from the known limiting cases and the asymptotic limit of $\lambda_D/L \to 0$. Our analysis can be readily extended for more complicated plasmas, and the resulting Bohm speed is consistent with the underlying plasma transport model. This last point accentuates the importance of an accurate plasma transport model that properly accounts for the kinetic nature of plasma transport within the Knudsen layer next to the wall, not only for bulk plasma transport, but also for the Bohm sheath constraint on wall-bound ion flow and energy flux.

---

[1] I. Langmuir, The interaction of electron and positive ion space charges in cathode sheaths, Phys. Rev. **33**, 954 (1929).

[2] L. Tonks and I. Langmuir, A general theory of the plasma of an arc, Phys. Rev. **34**, 876 (1929).

[3] M. A. Lieberman and A. J. Lichtenberg, *Principles of Plasma Discharges and Materials Processing*, 2nd ed. (Wiley-Interscience, New York, 2005).

[4] P. C. Stangeby, *The Plasma Boundary of Magnetic Fusion Devices* (Taylor & Francis, London, 2000).

[5] A. Loarte *et al.* (the ITPA Scrape-off Layer and D. P. T. Group), Chapter 4: Power and particle control, Nucl. Fusion **47**, S203 (2007).

[6] D. E. Hastings and H. B. Garrett, *Spacecraft-Environment Interactions* (Cambridge University Press, Cambridge, UK, 1996).

[7] S. T. Lai, *Fundamentals of Spacecraft Charging: Spacecraft Interactions with Space Plasmas* (Princeton University Press, Princeton, NJ, 2011).

[8] D. Bohm, The characteristics of electrical discharges in magnetic fields, *Qualitative Description of the Arc Plasma in a Magnetic Field* (McGraw-Hill, New York, 1949).

[9] E. R. Harrison and W. B. Thompson, The low pressure plane symmetric discharge, Proc. Phys. Soc. **74**, 145 (1959).

[10] K.-U. Riemann, The Bohm criterion and sheath formation, J. Phys. D **24**, 493 (1991).

[11] K.-U. Riemann, The Bohm criterion and boundary conditions for a multicomponent system, IEEE Trans. Plasma Sci. **23**, 709 (1995).

[12] S. D. Baalrud and C. C. Hegna, Kinetic theory of the presheath and the Bohm criterion, Plasma Sources Sci. Technol. **20**, 025013 (2011).

[13] R. M. Crespo and R. N. Franklin, Examining the range of validity of the Bohm criterion, J. Plasma Phys. **80**, 495 (2014).

[14] S. D. Baalrud, B. Scheiner, B. Yee, M. Hopkins, and E. Barnat, Extensions and applications of the Bohm criterion, Plasma Phys. Controlled Fusion **57**, 044003 (2015).

[15] V. A. Godyak, R. B. Piejak, and B. M. Alexandrovich, Probe diagnostics of non-Maxwellian plasmas, J. Appl. Phys. **73**, 3657 (1993).

[16] J. E. Allen, A note on the generalized sheath criterion, J. Phys. D **9**, 2331 (1976).

[17] R. C. Bissell and P. C. Johnson, The solution of the plasma equation in plane parallel geometry with a Maxwellian source, Phys. Fluids **30**, 779 (1987).

[18] K.-U. Riemann, Plasma-sheath transition in the kinetic Tonks-Langmuir model, Phys. Plasmas **13**, 063508 (2006).

[19] K.-U. Riemann, Comment on 'kinetic theory of the presheath and the Bohm criterion', Plasma Sources Sci. Technol. **21**, 068001 (2012).

[20] S. D. Baalrud and C. C. Hegna, Reply to comment on 'kinetic theory of the presheath and the Bohm criterion', Plasma Sources Sci. Technol. **21**, 068002 (2012).

[21] V. A. Godyak and N. Sternberg, Smooth plasma-sheath transition in a hydrodynamic model, IEEE Trans. Plasma Sci. **18**, 159 (1990).

[22] R. N. Franklin, You cannot patch active plasma and collisionless sheath, IEEE Trans. Plasma Sci. **30**, 352 (2002).

[23] I. D. Kaganovich, How to patch active plasma and collisionless sheath: A practical guide, Phys. Plasmas **9**, 4788 (2002).

[24] V. Godyak and N. Sternberg, Good news: You can patch active plasma and collisionless sheath, IEEE Trans. Plasma Sci. **31**, 303 (2003).

[25] K.-U. Riemann, Kinetic analysis of the collisional plasma–sheath transition, J. Phys. D **36**, 2811 (2003).

[26] R. N. Franklin, Where is the sheath edge?, J. Phys. D **37**, 1342 (2004).

[27] R. N. Franklin and J. R. Ockendon, Asymptotic matching of plasma and sheath in an active low pressure discharge, J. Plasma Phys. **4**, 371 (1970).

[28] N. Sternberg and V. Godyak, On asymptotic matching and the sheath edge, IEEE Trans. Plasma Sci. **31**, 665 (2003).

[29] X. Z. Tang, Kinetic magnetic dynamo in a sheath-limited high-temperature and low-density plasma, Plasma Phys. Controlled Fusion **53**, 082002 (2011).

[30] R. Chodura and F. Pohl, Hydrodynamic equations for anisotropic plasmas in magnetic fields. II. Transport equations including collisions, Plasma Phys. **13**, 645 (1971).

[31] X.-Z. Tang and Z. Guo, Critical role of electron heat flux on Bohm criterion, Phys. Plasmas **23**, 120701 (2016).

[32] X.-Z. Tang and Z. Guo, Kinetic model for the collisionless sheath of a collisional plasma, Phys. Plasmas **23**, 083503 (2016).

[33] B. B. K. J. Bowers, B. J. Albright, and T. Kwan, Ultrahigh performance three-dimensional electromagnetic relativistic kinetic plasma simulation, Phys. Plasmas **10:1**, 183 (2008).

[34] See Supplemental Material http://link.aps.org/supplemental/10.1103/PhysRevLett.128.085002 for the plasma profile and a comparison of simulation data with the collisional closure of Chodura and Pohl, which includes Refs. [29,30,35].

[35] T. Takizuka and H. Abe, A binary collision model for plasma simulation with a particle code, J. Comput. Phys. **25**, 205 (1977).

[36] Chodura and Pohl's collisional closure captures the trend but is less accurate than closure flux from kinetic simulations in predicting the Bohm speed, as expected.

[37] Z. Guo and X.-Z. Tang, Ambipolar Transport via Trapped-Electron Whistler Instability Along Open Magnetic Field Lines, Phys. Rev. Lett. **109**, 135005 (2012).

[38] Z. Guo and X.-Z. Tang, Parallel Heat Flux from Low to High Parallel Temperature Along a Magnetic Field Line, Phys. Rev. Lett. **108**, 165005 (2012).

[39] The nominal sheath Knudsen number is computed with initial plasma parameters for an isotropic plasma before the sheath is dynamically formed with absorbing walls and an upstream source. The local sheath Knudsen number is computed with local plasma parameters after the steady-state sheath is established, so it varies with position.